Phytochemicals and cyclodextris based-Pickering emulsions: natural potentiators of antibacterial, antifungal and antibiofilm Activity

Loïc Leclercq, Jérémie Tessier, Grégory Douyère, Véronique Nardello-Rataj, Andreea R. Schmitzer

Phytochemicals and cyclodextrins based- Pickering emulsions: natural potentiators of antibacterial, antifungal and antibiofilm activity

Loïc Leclercq,*[a] Jérémie Tessier,[b] Grégory Douyère,[a] Véronique Nardello-Rataj,[a] Andreea R. Schmitzer*[b]

[a] Univ. Lille, CNRS, Centrale Lille, Univ. Artois, UMR 8181 - UCCS - Unité de Catalyse et Chimie du Solide, 59000 Lille, France.

[b] Université de Montréal, Département de Chimie, CP 6128 Succursale Centre-Ville, H3C3J7, Montréal, Québec, Canada.

KEYWORDS Colloidal tectonics, Pickering emulsions, Phytochemicals, Cyclodextrins, Antimicrobial, Antibiofilm, Synergy

ABSTRACT: We present self-assembled Pickering emulsions containing biocidal phytochemical oils (carvacrol and terpinen-4-ol) and β-cyclodextrin able to potentiate the antimicrobial and antibiofilm activity of miconazoctylium bromide. Carvacrol-containing emulsion is two-fold more sensitive against *C. albicans* and *S. aureus* and highly active against *E. coli*, compared to the commercial cream containing miconazole nitrate. Moreover, this emulsion shows a synergistic effect against fungi, additive responses against bacteria and remarkable staphylococcal biofilm eradication. These results are associated to membrane permeabilization, enzymes inhibition and accumulation of reactive oxygen species in the microorganisms.

INTRODUCTION

Invasion of an organism by pathogens (bacteria, fungi, *etc*.) can cause health problems and even lead to death. Although hosts can react using their immune system, medications are widely prescribed to fight infectious diseases.[1] However, as the drug/target interaction is very selective and specific, antibiotics are generally active on bacteria but not on fungi, and *vice versa*.[2] Therefore, antifungals and antibiotics are used to fight fungi and bacteria, respectively. Unfortunately, as fungal infections can be superinfected with bacteria, antifungal therapy can lead to bacterial overgrowth.[3] Conversely, increased fungal microbiota growth is a common side effect of antibiotic therapy.[4] This is particularly vivid in immune-compromised patients for whom superficial infections, frequently caused by *Candida albicans*, can lead to oesophagus candidiasis or candidemia (the fourth cause of blood infections in the United States).[5] Moreover, debilitated patients are more at risk to contract hospital-acquired infections: Gram-negative bacteria (*e.g. Escherichia coli*) are estimated to account for two-thirds of the 25,000 hospital deaths per year in Europe.[6] The repeated exposure to antimicrobials may be an aggravating factor, as increasing selective pressure results in the emergence of resistant microorganisms, *e.g.* methicillin-resistant *Staphylococcus aureus*, *MRSA* (Gram-positive).[7] Furthermore, the formation of biofilms (accretion of microorganisms) results in more resistant infections to antimicrobials leading to chronic diseases.[8] For example, *S. aureus* form biofilms responsible for over 50,000 deaths annually in the United States.[9-10]

In this context, antimicrobials able to eradicate biofilms with large antibacterial and antifungal spectrum are necessary.[11-15] Among the numerous commercially employed antimicrobials, miconazole nitrate, [HMC][NO_3], responds partially to this request.[16] Indeed, it is active against a wide range of fungi and Gram-positive bacteria. Its antifungal activity is due to the inhibition of lanosterol 14-α-demethylase, involved in the ergosterol synthesis.[17] Since ergosterol is a major constituent of the fungal membrane, its depletion and the accumulation of toxic precursors result in growth inhibition. Additionally, [HMC][NO_3] induce generation and accumulation of reactive oxygen species (ROS).[18] These ROS act as nitric oxide dioxygenase inhibitors leading to significant cellular structural damage with lethal effects.[19] Although [HMC][NO_3] was inefficacious against Gram-negative bacteria and biofilms, its *N*-alkylation with *n*-octyl bromide was found to boost its antimicrobial activity.[20]

Herein, we decided to both formulate and potentiate the activity of miconazoctylium bromide, [C_8MC][Br] using two phytochemicals known to permeabilize microbial membranes: carvacrol[21-24] and terpinen-4-ol (Figure 1).[25-27]

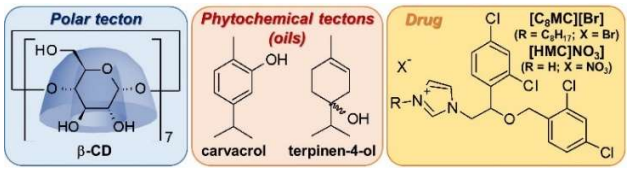

Figure 1. Structure and abbreviation of compounds used in this work.

These two liquid compounds, largely insoluble in water and toxic to microbial cells, can be used to obtain aqueous biphasic systems in which the phytochemical oils were used as organic solvents for [C_8MC][Br].[21-27] These water/oil systems in the presence of β-cyclodextrin (β-CD) can be used to build up drug delivery platforms based on Pickering emulsions using the colloidal tectonics concept.[28-31] In these media, host-guest interactions between polar and phytochemical tectons (CD and oil) lead to "amphiphilic" structured particles which adsorb at

the water/oil interface leading to Pickering emulsions.[28] These drug delivery systems can be charged with azole based drugs by direct solubilization in the phytochemical oil phase. Getting them is fairly easy, inexpensive and with the great advantage of avoiding the use of petro-sourced molecular surfactants or modified silica nanoparticles subject to controversy.[28] Regarding their activity, when the phytochemical oils are used in combination with [C_8MC][Br], it is expected to obtain a synergy in terms of antimicrobial and antibiofilm activities, due to cumulative membrane damages. These formulations could then be highly helpful for clinical applications, since a boosted antimicrobial allows: (*i*) a faster eradication of pathogens, (*ii*) a shorter treatment time, and (*iii*) a weaker spread of resistant pathogens *via* a complete and broad-spectrum eradication.[32-33]

EXPERIMENTAL SECTION

General Information. All chemicals were purchased from Sigma-Aldrich. NMR spectra were recorded in deuterated solvents at 400 MHz on Bruker spectrometer. The purity of final compounds used in biological assays was determined by ESI/LC-MS analysis (≥ 95%). Strains used were methicillin-resistant *S. aureus* ATCC 43300, *E. coli* ATCC 25922 and *C. albicans* SC5314. Sterile water was used in all experiments performed in triplicate.

Synthesis of miconazoctylium bromide. Miconazole (100 mg, 0.24 mmol) and *n*-octylbromide (125 µL, 0.72 mmol) was refluxed 2 h in MeCN (1 mL). The solvent was evaporated and the residue was suspended into EtOAc to remove any trace of octylbromide. Evaporation of the residual solvent afforded the salt as a white powder (135 mg, 0.22 mmol, 93%). ^{1}H NMR (400 MHz, $CDCl_3$) δ 10.51 (s, 1H), 7.49 (d, J = 8.3 Hz, 1H), 7.46-7.43 (m, 2H), 7.34-7.26 (m, 3H), 7.23-7.19 (m, 2H), 5.21 (dd, J = 7.5, 4.3 Hz, 1H), 4.74-4.60 (m, 2H), 4.51 (d, J = 11.9 Hz, 1H), 4.42 (d, J = 12.0 Hz, 1H), 4.29 (dh, J = 20.9, 7.3, 6.9 Hz, 2H), 1.91-1.80 (m, 2H), 1.26 (d, J = 20.4 Hz, 10H), 0.87 (t, J = 6.7 Hz, 3H). ; ^{13}C NMR (101 MHz, $CDCl_3$) δ 138.64, 135.93, 135.02, 134.28, 133.77, 132.86, 132.22, 131.49, 130.14, 129.39, 129.30, 128.37, 127.71, 122.57, 121.27, 76.18, 68.46, 53.25, 50.44, 31.80, 30.38, 29.14, 29.05, 26.36, 22.71, 14.19; HRMS : (ESI) calcd. for [M+] $C_{26}H_{31}Cl_4N_2O$: 527.1185, found 527.1194; IR (neat, cm^{-1}) 3007.9, 2927.5, 2926.5, 2854.5, 1646.7, 1587.7, 1561.3, 1467.4, 1379.8, 1338.7, 1298.0, 1222.8, 1191.2, 1145.5, 1095.9; M.P.: 131-134 °C.

Emulsion preparation and phase diagram. Oil and water were weighed before adding β-CD. Note that, if appropriated, drugs were diluted in oil. The emulsification was performed using Vortex-Genie 2 (3,200 rpm, 90 s, 25 °C, Scientific Industries Inc., USA). The type of emulsion was determined by conductivity measurement. The phase diagrams were obtained by visual and microscopic observations.

Microscopy. Optical microphotographs of the samples were obtained using a light microscope (Standard 25 ICS, Zeiss GmbH, Germany) coupled with a CCD camera. The microphotographs were analysed with ImageJ (NIH, USA) and the distribution function was obtained by treatment of at least 250 individual measurements with log-normal function using OriginPro 8® software (OriginLab Corp., USA). The morphology of the complexes was investigated by SEM (JSM-7800F LV, JEOL Ltd., Japan) operating at 2 KV for carvacrol and terpinen-4-ol complexes, and 5 KV for the complex formed with paraffin oil. The observations were performed by depositing the samples onto a carbon conductive adhesive tape stuck on a stub after air-drying and chromium coating. WETSEM observations of the emulsion were carried out with QX-102 capsules (Quantomix Ltd., Israel). The sample preparation proceeded as follow: 15 µL of sample were deposited in the liquid dish of the capsule and sealed with the stub. The beam was focused on the metal support grid with the SE detector before changing to the BSE detector to observe the sample. WETSEM photographs were analyzed with ImageJ to obtain 3D views.

X-ray powder diffraction. The data were collected on a Bruker D8 Advance, Bragg-Brentano diffractometer (Cu Kα radiation λ = 1.54056 Å) equipped with a LynxEye detector. Experiments were conducted at room temperature, over the 3-40° 2θ range with a 0.02° step size and counting time of 5 s. Sample diffracting volume was about 3 cm^2.

Differential scanning calorimetry. The measurements were performed on a DSC-Q1000 (TA Instruments, USA). About 10 mg of product were sealed in a Tzero Pan with a hermetic lid with pin hole and heated from 25 to 550 °C at a heating rate of 5 °C/min.

Multiple light scattering. The stability of emulsions was evaluated at 25 °C by multiple light scattering using Turbiscan Lab Expert (Formulaction, USA). The samples were placed in cylindrical glass tubes and the analysis was carried out as a variation of backscattering (ΔBS) profiles. Measurements were carried out using a pulsed near-IR light-emitting diode (LED) at 880 nm. Two different synchronous optical sensors received the light transmitted through and backscattered by samples at 180° and 45° with respect to the incident radiation, respectively. The two sensors scanned the entire sample height. Experimental data were correlated in percentage to the light flux of two standards: polystyrene latex suspension (absence of transmission and maximum backscattering) and silicon oil (maximum transmission and absence of backscattering).

Rheological study. Rheological properties of emulsions were evaluated using a Malvern Kinexus (Malvern Instruments, UK) equipped with parallel plate geometry under controlled temperature. The diameter of the plates was 20 mm and the gap was 1 mm. The temperature was controlled using a Peltier temperature control device located below the lower plate with an accuracy of 0.01 °C. Stress-controlled measurements were performed imposing a logarithmic stress ramp increase followed by a reverse stress decrease from 0 to 500 Pa.s.

Antimicrobial activity. Activity was determined using inhibition area on LB-agarose plates at 37 °C. The bacteria or yeast solution (OD = 0.1-0.15 at 600 nm) were spread onto LB-agar plates and incubated for 15 minutes at 37 °C for maximal absorption. One µL of each emulsion was then plated on the infected agar plate and incubated for 12h at 37 °C for bacteria and 30 °C for yeast. The area of inhibition for each formulation was then measured. The sterility tests used (LB only) were streaked onto LB-agar plates as an overall negative-control and infected plates without emulsion were streaked onto LB-agar plates as an overall positive-control.

Biofilm disruption. Bacteria were incubated in LB medium at 37 °C for 5 h and diluted in LB medium to the desired final concentration (OD = 0.1-0.15 at 600 nm). After an incubation of 12 h in 8-well chambers, the growth media was removed via pipetting and the resulting biofilms were washed 2 times with 0.9% NaCl solution to remove the remaining planktonic cells.

Biofilms were labelled with *Live/Dead* after 1 h exposition with different emulsions. Negative Control: DMSO (final concentration not exceeding 10% volume). Positive Control: 70% ethanol (20 min exposure). Biofilms stained with FilmTracer™ LIVE/DEAD® Biofilm viability kit (Molecular Probes, Life Technologies Ltd.). Briefly, a working solution of fluorescent stains was prepared by adding 1 µL of SYTO9® stain and 1 µL of propidium iodide (PI) stain to 1 mL of filter-sterilized water. Two hundred µL of staining solution were deposited on each well of an 8-well chambered coverglass, after 15 min at room temperature in the dark, samples were washed with sterile saline (0.9% NaCl) from base of the support material. Then, biofilms were examined with a confocal laser microscope (Leica model TCS SP5; Leica Microsystems CMS GmbH, Germany) using a 20x dry objective (HC PL FLUOTAR 20.0 × 0.50 DRY). A 488 nm laser line was used to excite SYTO® 9, while the fluorescent emission was detected from 500 to 540 nm. PI was sequentially excited with 561 nm laser line and its fluorescent emission was detected from 600 to 695 nm. The images acquired by confocal laser microscope were processed through a segmentation algorithm using Fiji (NIH, USA).

RESULTS

It is noteworthy that, in the following discussion, liquid paraffin served as reference because it is a widely used solvent in many commercial medicated creams and it is known to easily produce Pickering emulsions in the presence of β-CD.[28,34] As expected, all the water/oil/β-CD (45/45/10 wt.%) systems provided whitish emulsions (Figure 2A).

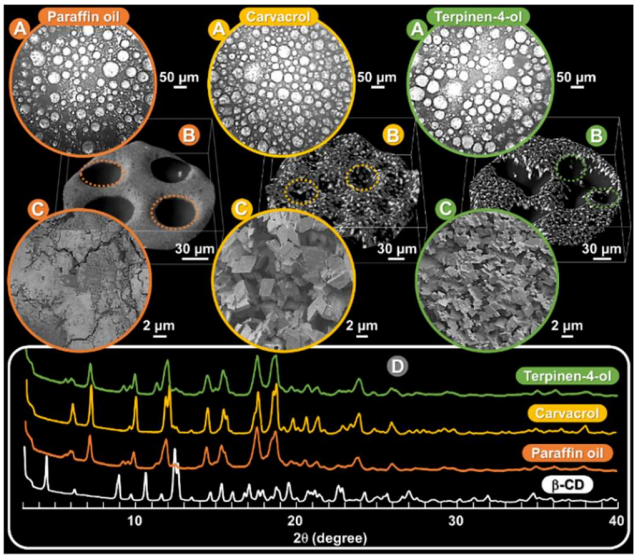

Figure 2. Observations of β-CD/water/oil emulsions (10/45/45 wt.%, 3,200 rpm, 90s, 25 °C) using optical microscope (**A**) and WETSEM (**B**) and of β-CD/oil complexes using dry SEM (**C**). The inset shows the X-ray powder diffraction patterns of dry powders (**D**).

The average droplet size is ≈ 35, 39, 36 µm (with a standard deviation, SD, of 5%) for paraffin, carvacrol and terpinen-4-ol, respectively (Figure S1). The electrical conductivity of the emulsions indicates an aqueous external phase. The morphology of the emulsions, in their native environment, were studied using a wet scanning electron microscopy (WETSEM, Figure 2B). The photographs show the presence of particles around the droplets in the continuous aqueous phase forming a 3D compact network (Figure S2). However, their centrifugation (4,000 rpm, 20 min) allows a separation of water, oil and a white powder. The dry powders were studied by SEM (Figure 2C). We observed a granular solid with paraffin oil and lamellar with carvacrol and terpinen-4-ol. Their sizes are in order: paraffin (≪ 1 µm) < terpinen-4-ol (≈ 1 µm) < carvacrol (≈ 4 µm). The ^{1}H NMR analysis in DMSO-d_6 of these powders suggests the formation of β-CD/oil complexes in equimolar ratios. The complexation is also supported by X-ray powder diffraction (XRD) as the diffraction patterns of precipitates are entirely different from that of the free β-CD (Figure 2D).[20] The XRD profiles suggest a well-ordered crystalline structure for all precipitates due to the presence of sharp peaks. Moreover, the differential scanning calorimetry thermogram of free β-CD shows two endothermic peaks around 141 and 303 °C, corresponding to the water release and to the melting of the β-CD, respectively, whereas for the precipitates, both peaks are shifted to lower temperatures due to the presence of the oil in the CD cavity instead of water molecules (Figure. S3).[35] All these results support the idea that β-CD and oil molecules, in the presence of water, allow the stabilization of Pickering emulsions *via* the formation of well-ordered crystalline β-CD/oil complexes.

The ternary phase diagrams of the β-CD/water/oil systems are shown in Figure 3. We always observed the formation of stable O/W emulsions (green and orange area), belted between O/W emulsions with excess oil phase (for high oil/water ratios) and O/W emulsions settled in the aqueous phase (for low oil/water ratios).[28,36] The other compositions provide water and oil phases with a large precipitated fraction.

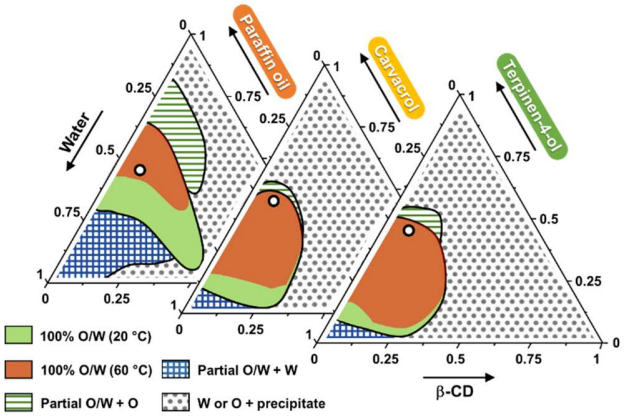

Figure 3. Ternary phase diagrams of the oil/water emulsion stabilized by β-CD at 25 °C. The composition is represented in weight fractions (3,200 rpm, 90s, 25 °C).

The location, range and stability of the self-assembled emulsions are clearly influenced by the oil polarity, the oil/water ratio as well as the β-CD concentration. Indeed, depending on the oil polarity, the stable O/W emulsion region moves towards the water corner and the two partial emulsion zones are reduced. These observations can be directly related to the modification of the oil polarity which leads to the modification of the stabilizing particles since they are obtained from host-guest interactions between oil and β-CD. The temperature effect on the stable emulsion area has been evaluated after a thermoregulation up to 60 °C. At 37 °C

(normal body temperature), the stable emulsion area is unaffected after two weeks for the three investigated oils. In contrast, at 60 °C, a reduction of the stable emulsion area is observed after 6h (orange area, Figure 2). This reduction is more significant for paraffin oil than for carvacrol or terpinen-4-ol due to the formation of a potential O-H•••O bond between the carvacrol or terpinen-4-ol and the β-CD leading to a better stabilization of the inclusion complexes and of the resulting crystalline particles as already reported with isopropyl myristate.[28] In addition, it is noteworthy that for a given oil/water ratio, the viscosity of the emulsions increases with the amount of β-CD. Moreover, for a given β-CD amount, the viscosity of the emulsions increases when the proportion of oil increases and the water decreases. Therefore, the best compromise between stability and viscosity of the emulsions is obtained for 10 wt.% of CD supplemented with 45% of water and 45% of oil (white circles in Figure 3).

For these particular compositions, the destabilization of the emulsions can be identified at an early stage by multiple light scattering (MLS) since the backscattered light (ΔBS) is related to droplet migration, droplet size and phases thickness (Figure 4A).[22]

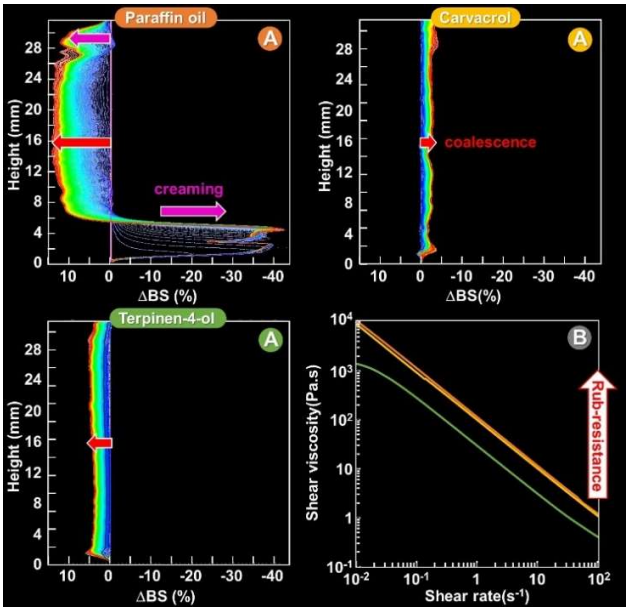

Figure 4. Backscattering (ΔBS) versus sample height and time at 25 °C (**A**) and shear viscosity as a function of shear rate (**B**) for β-CD/water/oil emulsions (10/45/45 wt.%, 3,200 rpm, 90s).

For paraffin, a creaming process was detected as the ΔBS over time decreases at the sample's bottom and increases at the top. An increase of ΔBS at the mid-height also indicates a coalescence phenomenon (droplet size variation).[36] For terpinen-4-ol and carvacrol, only coalescence was observed. However, as all these destabilization mechanisms have an impact on ΔBS over time, the sample with the highest variation is the less stable: the qualitative stability being in order: paraffin ≪ terpinen-4-ol < carvacrol. This phenomenon is dependent on the particle sizes since the larger ones offer a better stabilization, probably due to the 3D compact network of particles observed around the droplets in the continuous aqueous phase, leading to more or less frozen media and forming an excellent protection against coalescence. No macroscopic phase separation was noticeable after 4 months for the three emulsions. This is characteristic of Pickering emulsions as the coalescence frequency depends on time, particle concentration and mixing intensity. Indeed, if the particle amount is initially insufficient to fully cover the interfaces, the droplets coalesce. Fortunately, as the total interfacial area between oil and water is progressively reduced during this process and the particles are irreversibly adsorbed, the surface coverage degree increases until coalescence is stopped.[29-31] Unlike surfactant-stabilized emulsions, this process is limited and cannot be considered as a true instability.[29-31] However, for paraffin, the creaming is undesirable because it causes difficulties to storage and handling. We performed a rheological study (Figure 4B). The prepared formulations are highly viscous under storage conditions, but exhibit low viscosity under shear rate and are suitable for topical applications, since their viscosity is inferior to 2 Pa.s at 100 s^{-1}.[28] Also, the rub-resistance of the creams are in order: terpinen-4-ol ≪ carvacrol < paraffin.

The emulsion oil phase was charged with liposoluble [HMC][NO_3] or [C_8MC][Br] (final composition: 45% in weight of water, 44% of oil, 10% of β-CD and 1% of drug). All the emulsions behave similarly giving monomodal, but slightly polydisperse emulsions. However, some discrepancies between the emulsions can observed: the emulsions loaded with [C_8MC][Br] provide the smallest droplets (17 to 26 µm; SD = 5%), whereas the droplet sizes when charged with [HMC][NO_3] remain the same as those without drug (35 to 39 µm; SD = 5%). These results indicate that the amphiphilic [C_8MC][Br] may interact with the O/W interface stabilized by the β-CD/oil particles. Indeed, [C_8MC][Br] alone provides unstable emulsions which coalesce in a few minutes, leading to phase separation. However, the shear viscosity as a function of the shear rate remains identical with or without drugs.

As all emulsions are suitable for topical applications, diffusion tests were performed to evaluate their efficiency against *MRSA*, *E. coli* and *C. albicans* (Figure 5). Uncharged paraffin and commercial emulsion (Monistat Derm™) were used for comparison.

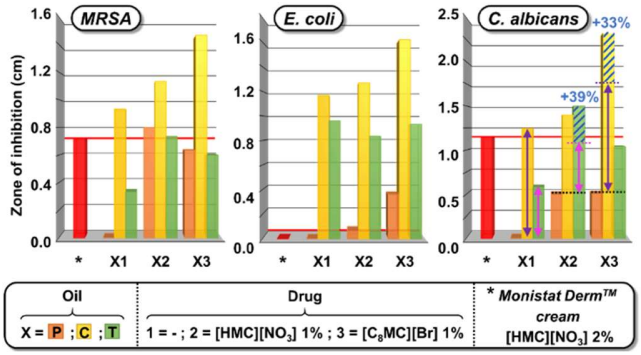

Figure 5. Zone of inhibition obtained by the diffusion method against *MRSA*, *E. coli* and *C. albicans* of the β-CD/water/oil emulsions compared to the commercial cream (Monistat Derm™; see the experimental section for more information).

As expected, the commercial cream is active against *MRSA* and *C. albicans*, but inactive against *E. coli*. The uncharged β-CD/water/paraffin oil (negative control, **P1**) is totally inactive against the three strains. In contrast, the two emulsions based on biocidal phytochemical oils (carvacrol, **C1**, and terpinen-4-

ol, **T1**) are active against all the pathogens. It is noteworthy that **C1** is the most active oil. Based on these observations, the emulsions formulated with paraffin were used to evaluate the antimicrobial action of [HMC][NO_3] or [C_8MC][Br] alone (**P2** and **P3**, respectively). Indeed, the pathogen susceptibility to [HMC][NO_3] and [C_8MC][Br] (**P2** and **P3**) was in order: *E. coli* < *C. albicans* < *MRSA*. As the addition of [HMC][NO_3] or [C_8MC][Br] to carvacrol or terpinen-4-ol oil can provides a route to potentiate the effect of the drug. The normalized biocidal factor (BF), expressed in %, was calculated as the ratio between the activity of drug/oil combination to the additive activities of each compound alone. Due to the standard deviations, a value of BF > 10% indicates a synergistic effect while a value BF < -10% means an antagonist effect. Finally, when -10% < BF < 10%, simple additivity is observed between the two components (Figure 6). According to these data, only the combination of [HMC][NO_3] to terpinen-4-ol (**T2**) and [C_8MC][Br] to carvacrol (**C3**) are synergetic against *C. albicans*. The other combinations result in antagonistic or additive effects against the three strains. Despite the fact that the normalized BF is quite superior for **T2** than **C3**, **T2** is not suitable to obtain broad-spectrum antimicrobial formulation due to the antagonistic effects observed against *MRSA* and *E. coli*. In contrast, the [C_8MC][Br]/carvacrol-based emulsion (**C3**) provides synergistic effect against *C. albicans* and additive responses against Gram-positive and Gram-negative bacteria. Moreover, this emulsion is two-fold more active against *C. albicans* and *S. aureus* than the commercial cream, with a high activity against *E. coli* compared to the completely inefficient commercial one. These antibacterial and antifungal activities may be the result of membrane permeabilization, enzymes inhibition and accumulation of ROS in the microorganisms (see above).

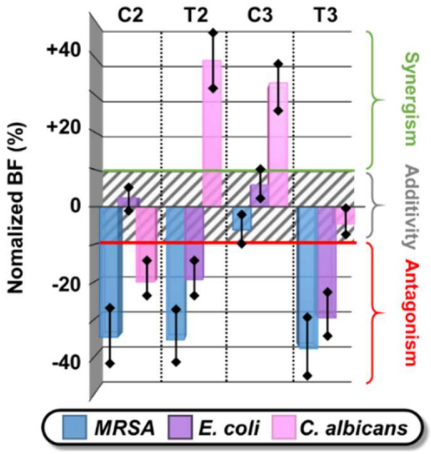

Figure 6. Normalized biocidal factor (BF) against *MRSA*, *E. coli* and *C. albicans* for β-CD/water/oil emulsions (oil = carvacrol, **C**, or terpinen-4-ol, **T**) combined with [HMC][NO_3] (**2**) or [C_8MC][Br] (**3**).

With these results in hand, we investigated the ability of the formulations to disrupt the *MRSA* biofilms. For this purpose, the pre-formed *MRSA* biofilms were treated with each formulation (1 µL) after one hour of incubation. The bacterial viability tests were performed using the commercially available fluorescence assay (*Bac*Light *Live/Dead*), composed of two fluorophores SYTO9® and propidium iodide, leading to the detection of alive intact cells (green) and permeabilized dead cells (red) (Figure 7).[37] [C_8MC][Br] aqueous solution (1 wt.%) shows a strong capacity to disrupt pre-formed *MRSA* biofilms, being able to kill bacteria more rapidly than ethanol (70%), probably due to its lipophilic character and ability to permeate cellular membranes.[20] As the viability of the biofilm can be perturbed by the viscosity of the Pickering emulsions, the paraffin-based formulations were used as control experiments. β-CD/water/paraffin emulsions uncharged or charged with [HMC][NO_3] (**P1** and **P2**, respectively) only show a local inhibition/destruction of the biofilm, but the majority of the bacteria are still alive in the biofilm. For paraffin-based formulations loaded with [C_8MC][Br] (**P3**), the formation of thicker stripes of colonies indicates an increased stress on bacteria and increased ROS production.[38] As indicated by the orange/yellow colour, about 75% of the bacteria in the biofilm were dead after 1h exposure with **P3**. Similar behaviours were observed with terpinen-4-ol-based formulations charged or not (**T1**, **T2** and **T3**). Moreover, bacterial mortality close to 100% was observed for all carvacrol-based emulsions. Therefore, the carvacrol emulsions act as very efficient biofilm-eradicating agents regardless of the drug used. However, more complete biofilm disruption was observed for the carvacrol-based emulsion charged with [C_8MC][Br] (**C3**).

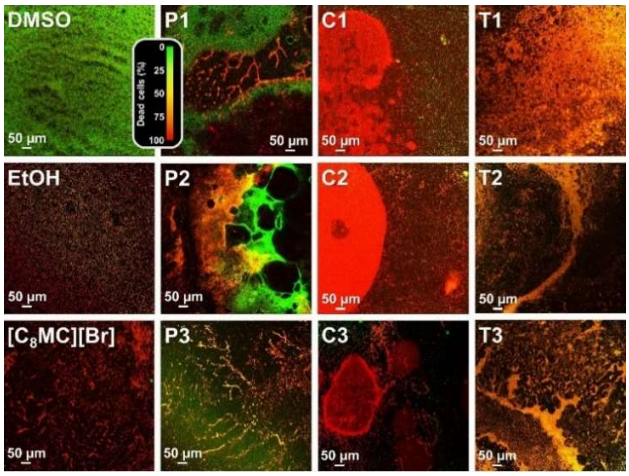

Figure 7. Pre-formed *MRSA* biofilms (*Live/Dead* stains) treated with 1 µL of β-CD/water/oil emulsions (oil = paraffin, **P**, carvacrol, **C**, or terpinen-4-ol, **T**) without (**1**) or with [HMC][NO_3] (**2**) or with [C_8MC][Br] (**3**) after incubation. Negative control (DMSO only). Positive controls (EtOH 70% and aqueous solution of [C_8MC][Br] 1 wt.%; see the experimental section for more information).

CONCLUSION

Self-assembled Pickering emulsion, obtained according to the so-called colloidal tectonics concept from commercially available and non-toxic raw materials (carvacrol and β-CD both approved by the Food and Drug Administration), can be used to improve the biocidal activity of miconazoctylium bromide. This very stable emulsion, in line with the current trend of simplifying formulas (without petro-sourced surfactants or modified silica nanoparticles), was shown to be two-fold more effective on C. albicans and MRSA than the commercial cream containing miconazole nitrate and showed high activity against E. coli, where the commercial one is completely inactive.[39-41] In addition, this emulsion was found to provide synergistic effect against *C. albicans* (30% more efficient than the additive effect). Finally, this system disrupted preformed *MRSA*

biofilms. Work is underway in our group to further develop these Pickering emulsions for clinical applications due to their broad-spectrum and fast action against bacteria and fungi, resistant strains and biofilms.

ASSOCIATED CONTENT

Supporting Information. Additional figures. This material is available free of charge via the Internet at http://pubs.acs.org.

AUTHOR INFORMATION

Corresponding Author

* E-mail: loic.leclercq@univ-lille.fr (L.L.)
* E-mail: ar.schmitzer@umontreal.ca (A.R.S.)

Author Contributions

The manuscript was written through contributions of all authors who approve the final version of the manuscript.

ACKNOWLEDGMENT

We gratefully acknowledge the Natural Sciences and Engineering Research Council of Canada (NSERC), the Chevreul Institute (FR 2638), the Ministère de l'Enseignement Supérieur et de la Recherche, the Région Hauts-de-France, the Université de Montréal and the Université de Lille for their financial support. We thank L. Burylo, J.-F. Dechézelles, A. Addad and A. Fadel for XRD, TEM and SEM measurements.

REFERENCES

(1) Taubes, G. The Bacteria Fight Back. *Science*, **2008**, *321*, 356-361.

(2) Wright, G. D. Antibiotics: A New Hope. *Chem. Biol.* **2012**, *19*, 3-10.

(3) Weidner, T.; Tittelbach, J.; Illing, T.; Elsner, P. Gram-Negative Bacterial Toe Web Infection: A Systematic Review. *Eur. Acad. Dermatol. Venereol.* **2018**, *32*, 39-47.

(4) Noverr, M. C.; Noggle, R. M.; Toews, G. B.; Huffnagle, G. B. Role of Antibiotics and Fungal Microbiota in Driving Pulmonary Allergic Responses. *Infect Immun.* **2004** *72*, 4996-5003.

(5) Pulimood, S.; Ganesan, L.; Alangaden, G.; Chandrasekar, P. Polymicrobial Candidemia. *Diagn. Microbiol. Infect. Dis.* **2002**, *44*, 353-357.

(6) Pollack, A. Rising Threat of Infections Unfazed by Antibiotics. *The New York Times*, Feb. 27, 2010.

(7) Davies, J.; Davies, D. Origins and Evolution of Antibiotic Resistance. *Microbiol. Mol. Biol. Rev.* **2010**, *74*, 417-433.

(8) Donlan, R. M. Biofilms: Microbial Life on Surfaces. *Emerg. Infect. Dis.* **2002**, *8*, 881-890.

(9) Worthington, R. J.; Richards, J. J.; Melander, C. Small Molecule Control of Bacterial Biofilms. *Org. Biomol. Chem.* **2012**, *10*, 7457-7474.

(10) Böttcher, T.; Kolodkin-Gal, I.; Kolter, R.; Losick, R.; Clardy, J. Synthesis and Activity of Biomimetic Biofilm Disruptors. *J. Am. Chem. Soc.* **2013**, *135*, 2927-2930.

(11) Jiao, Y.; Tay, F. R.; Niu, L.; Chen, J. Advancing Antimicrobial Strategies for Managing Oral Biofilm Infections. *Int. J. Oral. Sci.* **2019**, *11*, 28.

(12) Lu, J.; Cokcetin, N. N.; Burke, C. M.; Turnbull, L.; Liu, M.; Carter, D. A.; Whitchurch, C. B.; Harry, E. J. Honey Can Inhibit and Eliminate Biofilms Produced by Pseudomonas aeruginosa. *Sci. Rep.* **2019**, *9*, 18160.

(13) Godefroi, E. F.; Heeres, J.; Van Cutsem, J.; Janssen, P. A. J. Preparation and Antimycotic Properties of Derivatives of 1-Phenethylimidazole. *J. Med. Chem.* **1969**, *12*, 784-791.

(14) Sung, J. P.; Jan, M.; Grendahl, G.; Fresno, M.; Levine, H. B. Intravenous and Intrathecal Miconazole Therapy for Systemic Mycoses. *West. J. Med.* **1977**, *126*, 5-13.

(15) Nenoff, P.; Koch, D.; Kruger, C.; Drechsel, C.; Mayser, P. New Insights on the Antibacterial Efficacy of Miconazole in vitro. *Mycoses*, **2017**, *60*, 552-557.

(16) Allen, D.; Wilson, D.; Drew, R.; Perfect, J. Azole Antifungals: 35 Years of Invasive Fungal Infection Management. *Expert. Rev. Anti. Infect. Ther.* **2015**, *13*, 787-798.

(17) Becher, R.; Wirsel, S.G. Fungal Cytochrome P450 Sterol 14α-demethylase (CYP51) and Azole Resistance in Plant and Human Pathogens. *Appl. Microbiol. Biotechnol.* **2012**, *95*, 825-840.

(18) Kobayashi, D.; Kondo, K.; Uehara, N.; Otokozawa, S.; Tsuji, N.; Yagihashi, A.; Watanabe, N. Endogenous Reactive Oxygen Species is an Important Mediator of Miconazole Antifungal Effect. *Antimicrob. Agents Chemother.* **2002**, *46*, 3113-3117.

(19) El Hammi, E.; Warkentin, E.; Demmer, U.; Limam, F.; Marzouki, N. M.; Ermler, U.; Baciou, L. Structure of Ralstonia eutropha Flavohemoglobin in Complex with Three Antibiotic Azole Compounds. *Biochemistry*, **2011**, *50*, 1255-1264.

(20) Tessier, J.; Schmitzer, A. R. Anti-staphylococcal Biofilm Activity of Miconazoctylium Bromide. *Org. Biomol. Chem.* **2018**, *16*, 4288-4294.

(21) Xu, J.; Zhou, F.; Ji, B. P.; Pei, R. S.; Xu, N. The Antibacterial Mechanism of Carvacrol and Thymol Against Escherichia coli. *Lett. Appl. Microbiol.* **2008**, *47*, 174-179.

(22) Sharifi-Rad, M.; Varoni, E.M.; Iriti, M.; Martorell, M.; Setzer, W. N.; Del Mar Contreras, M.; Salehi, B.; Soltani-Nejad, A.; Rajabi, S.; Tajbakhsh, M.; Sharifi-Rad, J. Carvacrol and Human Health: A Comprehensive Review. *Phytother. Res.* **2018**, *32*, 1675-1687.

(23) Memar, M. Y.; Raei, P.; Alizadeh, N.; Akbari, A.; Masoud, K.; Hossein, S. Carvacrol and Thymol: Strong Antimicrobial Agents Against Resistant Isolates. *Rev. Med. Microbiol.* **2017**, *28*, 63-68.

(24) Khan, I.; Bahuguna, A.; Kumar, P.; Bajpai, V. K.; Kang, S. C. Antimicrobial Potential of Carvacrol against Uropathogenic Escherichia coli via Membrane Disruption, Depolarization, and Reactive Oxygen Species Generation. *Front Microbiol.* **2017**, *8*, 2421.

(25) Carson, C. F.; Riley, T. V. Antimicrobial Activity of the Major Components of the Essential Oil of Melaleuca alternifolia. *J. Appl. Bacteriol.* **1995**, *78*, 264-269.

(26) Carson, C. F.; Hammer, K. A.; Riley, T. V. Melaleuca alternifolia (Tea Tree) Oil: a Review of Antimicrobial and Other Medicinal Properties. *Clin. Microbiol. Rev.* **2006**, *19*, 50-62.

(27) Zhang, Y.; Feng, R.; Li, L.; Zhou, X.; Li, Z.; Jia, R.; Song, X.; Zou, Y.; Yin, L.; He, C.; Liang, X.; Zhou, W.; Wei, Q.; Du, Y.; Yan, K.; Wu, Z.; Yin, Z. The Antibacterial Mechanism of Terpinen-4-ol Against Streptococcus agalactiae. *Curr. Microbiol.* **2018**, *75*, 1214-1220.

(28) Leclercq, L.; Nardello-Rataj. V. Pickering Emulsions Based on Cyclodextrins: A Smart Solution for Antifungal Azole Derivatives Topical Delivery. *Eur. J. Pharm. Sci.* **2016**, *82*, 126-137.

(29) Leclercq, L. Get Beyond Limits: From Colloidal Tectonics Concept to the Engineering of Eco-Friendly Catalytic Systems. *Front. Chem.* **2018**, *6*, 168.

(30) Yang, B.; Leclercq, L.; Schmitt, V.; Pera-Titus, M.; Nardello-Rataj, V. Colloidal Tectonics for Tandem Synergistic Pickering Interfacial Catalysis: Oxidative Cleavage of Cyclohexene Oxide into Adipic Acid. *Chem. Sci.* **2019**, *10*, 501-507.

(31) Leclercq, L.; Douyère, G.; Nardello-Rataj, V. Supramolecular Chemistry and Self-Organization: A Veritable Playground for Catalysis. *Catalysts*, **2019**, *9*, 163.

(32) Acar, J. F. Antibiotic Synergy and Antagonism. *Med. Clin. North Am.* **2000**, *84*, 1391-1406.

(33) Leekha, S.; Terrell, C. L.; Edson, R. S. General Principles of Antimicrobial Therapy. *Mayo Clin. Proc.* **2011**, *86*, 156-167.

(34) Hashizaki, K.; Kageyama, T.; Inoue, M.; Taguchi, H.; Ueda, H.; Saito, Y. Study on Preparation and Formation Mechanism of n-Alkanol/Water Emulsion Using α-Cyclodextrin. *Chem. Pharm. Bull.* **2007**, *55*, 1620-1625.

(35) Mohandoss, S.; Stalin, T. Photochemical and Computational Studies of Inclusion Complexes Between β-Cyclodextrin and 1,2-Dihydroxyanthraquinones. *Photochem. Photobiol. Sci.* **2017**, *16*, 476-488.

(36) Leclercq, L.; Company, R.; Mühlbauer, A.; Mouret, A.; Aubry, J.-M.; Nardello-Rataj, V. Versatile Eco-Friendly Pickering Emulsions Based on Substrate/Native Cyclodextrin Complexes: a Winning Approach for Solvent-Free Oxidations. *ChemSusChem*, **2013**, *6*, 1533-1540.

(37) Berney, M.; Hammes, F.; Bosshard, F.; Weilenmann, H. U.; Egli, T. Assessment and Interpretation of Bacterial Viability by Using the LIVE/DEAD BacLight Kit in Combination with Flow Cytometry. *Appl. Environ. Microbiol.* **2007**, *73*, 3283-3290.

(38) Giuliodori, A. M.; Gualerzi, C. O.; Soto, S.; Vila, J.; Tavio, M. M. Review on Bacterial Stress Topics. *Ann. N. Y. Acad. Sci.* **2007**, *1113*, 95-104.

(39) Doost, A. S.; Stevens, C. V.; Claeys, M.; Van Der Meeren, P. Fundamental Study on the Salt Tolerance of Oregano Essential Oil-in-Water Nanoemulsions Containing Tween 80. *Langmuir* **2019**, *35*, 10572-81.

(40) Kaliamurthi, S.; Selvaraj, G.; Hou, H.; Li, Z.; Wei, Y.; Gu, K.; Wei, D. Synergism of essential oils with lipid based nanocarriers: emerging trends in preservation of grains and related food products. *Grain Oil Sci. Technol.* **2019**, *2*, 21-26.

(41) Doost, A. S.; Nikbakht Nasrabadi, M. N.; Kassozi, V.; Nakisozi, H.; Van der Meeren, P. Recent advances in food colloidal delivery systems for essential oils and their main components. *Trends Food Sci. Technol.* **2020**, In Press.

Table of Contents